

Complete power spectrum for an induced gravity open inflation model

Juan García-Bellido

*Astronomy Centre, University of Sussex, Falmer, Brighton BN1 9QH, United Kingdom,
and Theory Division, CERN, CH-1211 Geneva 23, Switzerland*

Andrew R. Liddle

Astronomy Centre, University of Sussex, Falmer, Brighton BN1 9QH, United Kingdom

(Received 23 October 1996)

We study the phenomenological constraints on a recently proposed model of open inflation in the context of induced gravity. The main interest of this model is the relatively small number of parameters, which may be constrained by many different types of observation. We evaluate the complete spectrum of density perturbations, which contains continuum subcurvature modes, a discrete supercurvature mode, and a mode associated with fluctuations in the bubble wall. From these, we compute the angular power spectrum of temperature fluctuations in the microwave background, and derive bounds on the parameters of the model so that the predicted spectrum is compatible with the observed anisotropy of the microwave background and with large-scale structure observations. We analyze the matter era and the approach of the model to general relativity. The model passes all existing constraints. [S0556-2821(97)05608-7]

PACS number(s): 98.80.Cq, 98.70.Vc

I. INTRODUCTION

The inflationary paradigm [1] not only provides a solution to the classical problems of the hot big bang cosmology, but also predicts an almost scale-invariant spectrum of metric perturbations which could be responsible for the observed anisotropy of the cosmic microwave background (CMB), as well as the origin of the large-scale structure. Present microwave background anisotropy experiments offer only weak constraints; for example, the Cosmic Background Explorer (COBE) satellite [2] gives a very accurate determination of the amplitude of large-angle anisotropies (which can be used to normalize theories) but only weakly constrains the shape of the spectrum. Information is beginning to come in on degree scales, and from combining microwave anisotropy constraints with those from large-scale structure, but the present situation still offers considerable freedom. However, we can expect this to change dramatically in the near future, especially with the launch of new-generation microwave anisotropy satellites MAP [3] and Planck [4] which promise to measure both cosmological parameters such as Ω_0 , H_0 , and Ω_B , and parameters associated with the primordial spectra to great accuracy [5]. It is, therefore, desirable to provide a variety of inflationary models with definite predictions, which could be used to test and exclude them.

Until recently, inflation was always associated with a flat universe, due to its ability to drive the spatial curvature so effectively to zero. However, it is now understood that inflation comprises a wider class of models, some of which may give rise to an open universe at present [6–8]. Observations suggesting a high value of the Hubble parameter, such as those using the Hubble Space Telescope [9], have motivated the idea of considering a low-density universe, in an attempt to make the age compatible with globular cluster ages. Most frequently, a cosmological constant is introduced to restore spatial flatness, but open inflation models (see Ref. [10] for an introduction) offer the alternative of a genuinely open

universe. Such models generically contain a field trapped in a false vacuum which tunnels to its true vacuum via nucleation of a single bubble, inside which a second period of inflation drives the universe to almost flatness. This way, one solves the homogeneity problem independently from the flatness problem, allowing for an open homogeneous universe inside the bubble.

In an open universe, the analysis of density perturbations and microwave anisotropies is considerably more complicated than that in the usual flat-space case. Early studies by Lyth and Stewart [11] and by Ratra and Peebles [12] evaluated the spectrum for slow roll models leading to an open universe, using the conformal vacuum as an initial condition. In the single-bubble models a different vacuum choice is appropriate, leading to a slightly different spectrum [13,7]. It was later realized, however, that extra perturbations, with discrete wave numbers, can also be generated. In all, three different types of perturbation have been identified: a continuous spectrum of modes with wave number k greater than the curvature scale, known as subcurvature modes; a supercurvature mode associated with the open de Sitter vacuum [13,14], and a mode associated with perturbations in the bubble-wall at tunneling [15–17]. The observed large-scale structures are due to the subcurvature modes, but large-angle microwave anisotropies are generated by all three types, with observations seeing the combined total anisotropy. The first computation of all three types of modes together for a particular model was made in Ref. [15] for arbitrary Ω_0 in the context of the two-field models of Linde and Mezhlumian [8]. Later on, a thorough calculation of all three contributions from the point of view of quantum field theory in open de Sitter space was carried out by Yamamoto *et al.* [17] (see also Ref. [18]). Here, we shall carry out a similar calculation for a different two-field model, for which we shall also discuss some of the implications of large-scale structure observations.

In addition to scalar metric perturbations, we expect open inflation to lead to the production of a gravitational wave spectrum, as in conventional inflationary models. Unfortunately, no one has yet formulated a method of calculating this spectrum even approximately, and so we shall not be able to consider them here. In chaotic inflation models, gravitational waves are negligible in the slow roll limit (see, e.g., Ref. [19]); one can hope that this is also true in the open inflation case, but that remains to be confirmed.

The particular open inflation model we shall study, introduced in Ref. [20], is based on the induced gravity Lagrangian [21]. The interest of this model is the relatively small number of parameters, which can be constrained by several different types of observation. The inflaton is a dilaton field, whose vacuum expectation value at the end of inflation determines the present value of the gravitational constant. We will constrain the model from CMB and large-scale structure observations, as well as ensuring that post-Newtonian and oscillating gravitational coupling bounds are satisfied.

II. THE MODEL

We consider the model of Ref. [20], with an induced gravity Lagrangian [21]

$$\mathcal{L} = \frac{1}{2} \xi \varphi^2 R - \frac{1}{2} \partial_\mu \varphi \partial^\mu \varphi + V(\varphi) + \mathcal{L}_{\text{mat}}. \quad (1)$$

The dilaton field φ determines the effective gravitational coupling, which is positive for $\xi > 0$. In the absence of a potential, this action corresponds to the usual Brans-Dicke action [22], where

$$\Phi = 8\pi\xi\varphi^2, \quad \omega = \frac{1}{4\xi}. \quad (2)$$

The Einstein and scalar field equations are [23,24]

$$-\xi\varphi^2 G_{\mu\nu} = g_{\mu\nu} V(\varphi) + \xi(\nabla_\mu \nabla_\nu - g_{\mu\nu} \nabla^2)\varphi^2 + [\partial_\mu \varphi \partial_\nu \varphi - \frac{1}{2} g_{\mu\nu} (\partial\varphi)^2] + T_{\mu\nu}, \quad (3)$$

and

$$\nabla^2 \varphi = -V'(\varphi) + \xi\varphi R, \quad (4)$$

where $G_{\mu\nu}$ is the Einstein tensor. Using the identities $G_{\mu\nu};{}^\nu = 0$ and $R_{\mu\nu} \nabla^\nu \Phi = \nabla_\mu (\nabla^2 \Phi) - \nabla^2 (\nabla_\mu \Phi)$, together with the φ equation of motion, we find that the energy-momentum tensor is conserved,

$$T_{\mu\nu};{}^\nu = 0, \quad (5)$$

even in the presence of a potential for the scalar field. Substituting R into the equation of motion of the scalar field, we obtain

$$\frac{1}{2} (1 + 6\xi) \nabla^2 \varphi^2 = 4V(\varphi) - \varphi V'(\varphi) + T^\lambda{}_\lambda. \quad (6)$$

We will consider a potential of the type [21,20]

$$V(\varphi) = \frac{\lambda}{8} (\varphi^2 - \nu^2)^2. \quad (7)$$

During a radiation-dominated era $T^\lambda{}_\lambda = 0$ and the scalar field will sit at its minimum; matching the present-day Planck mass demands,

$$8\pi\xi\nu^2 = m_{\text{Pl}}^2. \quad (8)$$

During a matter era, the scalar field oscillates around its minimum with a large frequency and negligible amplitude, passing all the tests associated with an oscillating gravitational coupling [25] as we will show in Sec. VII.

III. INDUCED GRAVITY OPEN INFLATION

In the induced gravity open inflation model [20], the initial period of inflation is driven by the false vacuum energy of a second scalar field σ . This energy density is able to hold the dilaton at a fixed location displaced from the minimum of its potential. After the false vacuum decays, the rolling of the dilaton to its minimum drives the second period of inflation necessary to give Ω_0 in the desired range.

A. False vacuum inflation

Initially, the scalar field σ is in its false vacuum. The details of its potential are not particularly important; we will parametrize them later. In the false vacuum, the universe expands driving the spatial curvature and any previous inhomogeneities to zero. Later on, the σ field tunnels to its true minimum at $V(\sigma) = 0$, via the production of a bubble.

The equations of motion of the dilaton field before and after the tunneling can be written as [20]

$$H^2 + 2H \frac{\dot{\varphi}}{\varphi} + \frac{K}{a^2} = \frac{1}{3\xi\varphi^2} \left[\frac{1}{2} \dot{\varphi}^2 + V(\varphi) + V(\sigma) \right], \quad (9)$$

$$\ddot{\varphi} + 3H\dot{\varphi} + \frac{\dot{\varphi}^2}{\varphi} = \frac{4V(\varphi) - \varphi V'(\varphi) + 4V(\sigma)}{(1 + 6\xi)\varphi}. \quad (10)$$

Here, $V(\sigma) = V_0$ in the false vacuum and vanishes in the true vacuum, while the curvature K is effectively zero before tunneling and is negative afterwards. The basis for the open inflation model is the existence of a stable static solution in the false vacuum [20], with

$$\varphi_{\text{st}}^2 = \nu^2 \left(1 + \frac{8V_0}{\lambda\nu^4} \right) \equiv \nu^2 (1 + \alpha), \quad (11)$$

$$H_{\text{st}}^2 = \frac{8\pi V_0}{3m_{\text{Pl}}^2}. \quad (12)$$

Its stability is best seen in the Einstein frame [20]. Under the transformations

$$dt = \frac{\nu}{\varphi} d\tilde{t}, \quad a(t) = \frac{\nu}{\varphi} \tilde{a}(\tilde{t}), \quad (13)$$

$$\frac{\phi}{\nu} = (1 + 6\xi)^{1/2} \ln \frac{\varphi}{\nu}, \quad (14)$$

the effective potential in the false vacuum becomes

$$U_F(\phi) = \frac{\lambda \nu^4}{8} \left[1 - 2 \frac{\nu^2}{\varphi^2} + (1 + \alpha) \frac{\nu^4}{\varphi^4} \right], \quad (15)$$

$$U'_F(\phi) = \frac{\lambda \nu^3}{2(1 + 6\xi)^{1/2}} \frac{\nu^2}{\varphi^2} \left[1 - (1 + \alpha) \frac{\nu^2}{\varphi^2} \right], \quad (16)$$

$$U''_F(\phi) = \frac{\lambda \nu^2}{1 + 6\xi \varphi^2} \frac{\nu^2}{\varphi^2} \left[2(1 + \alpha) \frac{\nu^2}{\varphi^2} - 1 \right], \quad (17)$$

where primes denote derivatives with respect to the Einstein-frame scalar field ϕ . It is clear that $U'_F(\phi_{st}) = 0$ at the static value, while the effective square mass is positive ensuring stability. At the static point, we have

$$H_F^2 = \frac{8\pi U_F}{3m_{Pl}^2} = \frac{\lambda \nu^2}{24\xi} \frac{\alpha}{1 + \alpha}, \quad (18)$$

$$m_F^2 \equiv U''_F(\varphi_{st}) = \frac{\lambda \nu^2}{1 + 6\xi} \frac{1}{1 + \alpha}, \quad (19)$$

where H_F is the rate of expansion of the universe in the Einstein frame and m_F is the mass of the ϕ field at the static point.

B. True vacuum inflation

Eventually, the σ field tunnels to its true vacuum by nucleating a bubble, inside which the universe inflates to almost flatness. A sufficiently low tunneling rate ensures that the bubble stays isolated [26,20]. After tunneling, the effective potential in the true vacuum, again in the Einstein frame, becomes

$$U_T(\phi) = \frac{\lambda \nu^4}{8} \left(1 - \frac{\nu^2}{\varphi^2} \right)^2, \quad (20)$$

$$U'_T(\phi) = \frac{\lambda \nu^3}{2(1 + 6\xi)^{1/2}} \frac{\nu^2}{\varphi^2} \left(1 - \frac{\nu^2}{\varphi^2} \right), \quad (21)$$

$$U''_T(\phi) = \frac{\lambda \nu^2}{1 + 6\xi} \frac{\nu^2}{\varphi^2} \left(2 \frac{\nu^2}{\varphi^2} - 1 \right). \quad (22)$$

The minimum of the potential is now at $\varphi = \nu < \varphi_{st}$, and the field slow rolls from φ_{st} driving a second stage of inflation. The dynamics of this situation were investigated long ago in Ref. [27]. The rate of expansion and effective mass in the true vacuum immediately after tunneling are

$$H_T^2 = \frac{8\pi U_T}{3m_{Pl}^2} - \frac{K}{a^2} = \frac{\lambda \nu^2}{24\xi} \left(\frac{\alpha}{1 + \alpha} \right)^2 - \frac{K}{a^2}, \quad (23)$$

$$m_T^2 \equiv U''_T(\varphi_{st}) = \frac{\lambda \nu^2}{1 + 6\xi} \frac{1 - \alpha}{(1 + \alpha)^2}. \quad (24)$$

The curvature term quickly becomes negligible as the second phase of inflation progresses.

For later use, we also define the usual slow roll parameters [19] soon after tunneling:

$$\epsilon \equiv \frac{m_{Pl}^2}{16\pi} \left(\frac{U'_T(\phi)}{U_T(\phi)} \right)^2 = \frac{8\xi}{1 + 6\xi} \frac{1}{\alpha^2}, \quad (25)$$

$$\eta \equiv \frac{m_{Pl}^2}{8\pi} \frac{U''_T(\phi)}{U_T(\phi)} = \frac{8\xi}{1 + 6\xi} \frac{1 - \alpha}{\alpha^2}. \quad (26)$$

The scalar field ϕ slow rolls down the effective potential given by Eq. (20) until it starts oscillating around its minimum and inflation ends. The value of ϕ at the end of inflation can be computed from the condition $-\dot{H}_T \approx H_T^2$ [or, equivalently, $\dot{\phi}^2 \approx U_T(\phi)$], giving

$$\varphi_{end}^2 = \nu^2 \left(1 + \frac{8\xi}{1 + 6\xi} \right) \equiv \nu^2 (1 + \beta). \quad (27)$$

The number of e -folds during the second stage of inflation from ϕ_{st} to ϕ_{end} can be computed in the Einstein frame:

$$\begin{aligned} N &= \frac{1}{\xi \nu^2} \int_{\phi_{end}}^{\phi_{st}} \frac{d\phi U_T(\phi)}{U'_T(\phi)} \\ &= \frac{1}{\beta} \left[\alpha - \beta - \ln \left(\frac{1 + \alpha}{1 + \beta} \right) \right]. \end{aligned} \quad (28)$$

In order to produce an open universe, the number of e -folds after tunneling has to be around $N = 60$, the precise number depending on the reheating temperature and other details of the post-inflationary evolution. We adopt the number 60 for definiteness. This gives a relation between the two dimensionless parameters α and β .

IV. METRIC PERTURBATIONS AND TEMPERATURE ANISOTROPIES

Quantum fluctuations of the inflaton field ϕ produce long-wavelength curvature perturbations; we will use \mathcal{R} to denote the curvature perturbation on comoving hypersurfaces (in the Einstein frame).

Open inflation generates three different types of modes: those that cross outside during the second stage of inflation and constitute a continuum of subcurvature modes; a discrete supercurvature mode associated with the open de Sitter vacuum, and a mode associated with the bubble-wall fluctuations at tunneling. The mode functions are eigenvalues of the Laplacian, with eigenvalue $-k^2$ where k is the wave number. Defining $q^2 = k^2 - 1$, the subcurvature modes then have positive q^2 and the other modes have negative q^2 . We label the former mode functions $\Pi_{q|l}(r)$ and the latter $\bar{\Pi}_{|q|l}(r)$. In Appendix A we give explicit forms for these; see also Ref. [28].

The spectrum $\mathcal{P}_{\mathcal{R}}(q)$ of the curvature perturbation can be defined from the mode expansion of \mathcal{R} by [14]

$$\langle \mathcal{R}_{q|lm} \mathcal{R}_{q'|l'm'} \rangle = \frac{2\pi^2}{q(q^2 + 1)} \mathcal{P}_{\mathcal{R}}(q) \delta(q - q') \delta_{ll'} \delta_{mm'}. \quad (29)$$

In order to compare with observations, we must compute the effect that such a perturbation has on the temperature of the CMB, expanded as usual in spherical harmonics

$$\frac{\Delta T}{T}(\theta, \phi) = \sum_{lm} a_{lm} Y_m^l(\theta, \phi). \quad (30)$$

The main contribution on large scales comes from the Sachs-Wolfe effect [29]. The complete angular power spectrum $C_l \equiv \langle |a_{lm}|^2 \rangle$ has contributions from the continuum of subcurvature modes, the supercurvature mode, and the bubble-wall mode,

$$C_l = C_l^{(C)} + C_l^{(S)} + C_l^{(W)}. \quad (31)$$

The contribution of each mode to the C_l is measured by a window function W_{ql} , given by [29]

$$5 W_{ql} = \Pi_{ql}(\eta_0) + 6 \int_0^{\eta_0} dr F'(\eta_0 - r) \Pi_{ql}(r), \quad (32)$$

for the subcurvature modes; the same expression with $\bar{\Pi}_{|q|l}$ gives the window function $\bar{W}_{|q|l}$ for the negative q^2 modes. Here,

$$F(\eta) = 5 \frac{\sinh^2 \eta - 3 \eta \sinh \eta + 4(\cosh \eta - 1)}{(\cosh \eta - 1)^3}, \quad (33)$$

gives the growth rate of perturbations during the matter era [30], and $\eta_0 = \text{arccosh}(2/\Omega_0 - 1)$ is the distance to the last scattering surface. The normalization of the contribution to the C_l is given in the expressions below.

A. Subcurvature modes

A detailed computation of the amplitude of the subcurvature modes gives the result [13,7,17]

$$\mathcal{P}_{\mathcal{R}}(q) = \coth(\pi q) \frac{8U_{\text{T}}}{3\epsilon m_{\text{Pl}}^4}, \quad (34)$$

where ϵ is the slow roll parameter defined earlier and we have dropped a small correction term from the change in mass during tunneling [17]. The $\coth(\pi q)$ factor can be interpreted as due to the initial transient behavior as the curvature term dies away.

Notice that Eq. (34) has only been derived in the case of a perfect de Sitter expansion after tunneling [17]. It seems very plausible that it also holds when there are deviations from de Sitter, where the right-hand side is to be evaluated when $k = aH$. This is the only simple formula which reduces to the correct result both for de Sitter expansion and in the flat-space limit (see, e.g., Ref. [31]) which must be attained after the curvature term has died away sufficiently.

Following normal practice, we describe the variation in the spectrum caused by the time variation of H and ϵ by a power law. Notice that this power law is superimposed on the \coth behavior, so the complete spectrum does not have a power-law form on very large scales. The power-law index of $\mathcal{P}_{\mathcal{R}}(q)/\coth(\pi q)$ can be derived in the usual way from the slow roll parameters as [19]

$$n - 1 = -6\epsilon + 2\eta = -\frac{8\xi}{1+6\xi} \frac{2(2+\alpha)}{\alpha^2}, \quad (35)$$

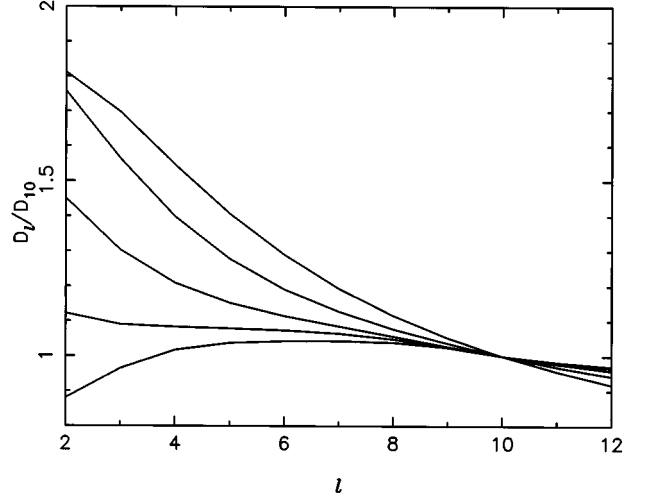


FIG. 1. The first 12 multipoles of the angular power spectrum associated with the continuum modes, normalized to the tenth multipole, for $\Omega_0 = 0.2, 0.3, 0.4, 0.5, 0.6$ as read from top to bottom at low l .

and gives the standard result in the flat-space limit where the \coth term in Eq. (34) equals unity. This expression is valid provided both ϵ and $|\eta|$ are much less than 1.

For later comparison, we write the spectrum as

$$\mathcal{P}_{\mathcal{R}}(q) = A_C^2 \coth(\pi q) [1 + q^2]^{(n-1)/2}, \quad (36)$$

where

$$A_C^2 = \frac{8U_{\text{T}}(\phi_{\text{st}})}{3\epsilon(\phi_{\text{st}})m_{\text{Pl}}^4} \quad (37)$$

is a measure of the amplitude at the $q=0$ limit. Formally, the spectrum diverges there, though not in a harmful way thanks to the window function given by Eq. (32).

For our model, Eq. (37) becomes

$$A_C^2 = \frac{\lambda}{(16\pi\xi)^2} \frac{1+6\xi}{6\xi} \left(\frac{\alpha^2}{1+\alpha} \right)^2. \quad (38)$$

The angular power spectrum for the continuum modes can be written as [13]

$$C_l^{(C)} = 2\pi^2 \int_0^\infty \frac{dq}{q(1+q^2)} \mathcal{P}_{\mathcal{R}}(q) W_{ql}^2. \quad (39)$$

We compute the angular power spectrum for different values of Ω_0 in the low-density range $0.2 \leq \Omega_0 \leq 0.6$. In Fig. 1 we show the first 12 multipoles, adopting the notation¹ $D_l = l(l+1)C_l$.

¹Our calculation only includes the Sachs-Wolfe effect, as is appropriate for computing the amplitude on the largest angular scales. We do not include the rise to the acoustic peak, caused by the first oscillation of the photon-baryon fluid, which is known to induce an effective extra tilt of around 0.15 [32]; see, for example, Fig. 8 in Ref. [33] (who only consider subcurvature modes).

The normalization to COBE for tilted open models has recently been given by Bunn and White [33], under the assumption that only the continuum modes are important. They specify a quantity δ_H , which measures the normalization of the present matter power spectrum. The preferred value depends on n and Ω_0 ; however, our model is nearly scale invariant, and the dependence on Ω_0 is quite weak and can be ignored at the accuracy we are working. Therefore, we take the value $\delta_H = 2 \times 10^{-5}$ regardless of Ω_0 . In an open universe δ_H is related to \mathcal{P}_R as [33]

$$\delta_H = \frac{2}{5} \mathcal{P}_R^{1/2} \frac{g(\Omega_0)}{\Omega_0}, \quad (40)$$

where $g(\Omega_0)$ is a function measuring the suppression in the growth perturbations relative to a critical-density universe, and \mathcal{P}_R is evaluated at around the tenth multipole where $\coth(\pi q) \approx 1$. The Ω_0 dependence can give a factor of up to 1.5 in the region of interest, but we can ignore it as we do not require such accuracy. Reproducing the amplitude of temperature anisotropies is the main constraint on the parameters of the model, and yields

$$\sqrt{\lambda} = 6 \times 10^{-3} \left(\frac{\xi^3}{1+6\xi} \right)^{1/2} \frac{1+\alpha}{\alpha^2}, \quad (41)$$

as found in Ref. [20]. This relation can readily be satisfied for reasonable values of the parameters [20].

B. Supercurvature mode

We now consider the contribution to the CMB anisotropies coming from the discrete supercurvature mode associated with the dilaton field ϕ . This mode appears in the open de Sitter spectrum when $m_F^2 < 2H_F^2$ in the false vacuum [13]. The tunneling field σ does not have this mode in its spectrum, since its mass in the false vacuum should be much larger than the rate of expansion in order to prevent tunneling via the Hawking-Moss instanton [8]. The wave number associated with this mode is given by

$$k^2 = 1 - \left[\left(\frac{9}{4} - \frac{m_F^2}{H_F^2} \right)^{1/2} - \frac{1}{2} \right]^2. \quad (42)$$

The amplitude of this mode is [18]

$$A_S^2 \approx \frac{8U_F}{3\epsilon m_{\text{Pl}}^4} = A_C^2 \frac{U_F}{U_T}, \quad (43)$$

where the normalization of A_S^2 is defined through the formula for the angular power spectrum of temperature anisotropies induced by this supercurvature mode; namely [17,18],

$$D_l^{(S)} \equiv l(l+1)C_l^{(S)} = 4\pi A_S^2 \bar{W}_{1l}^2. \quad (44)$$

Figure 2 shows the first 12 multipoles, showing quite a complicated dependence. For example, it is not automatic that the quadrupole receives the biggest contribution [34].

More important than the shape is the amplitude of these anisotropies relative to the subcurvature ones. We will compare their contributions in Sec. V.

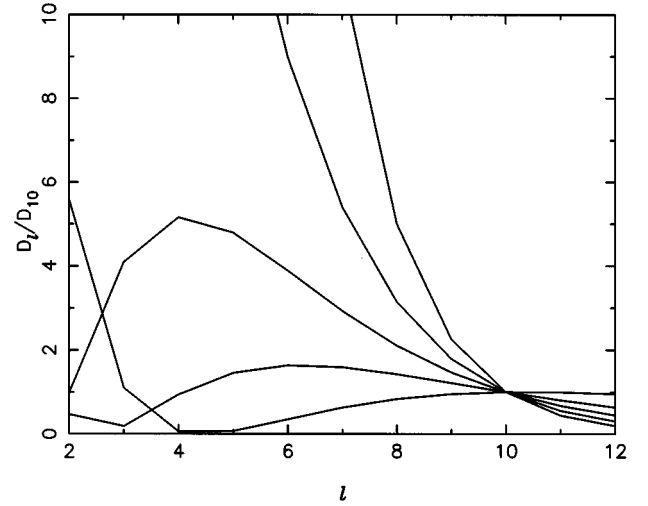


FIG. 2. As Fig. 1, but for the discrete supercurvature mode, showing $\Omega_0 = 0.6, 0.5, 0.4, 0.3, 0.2$, reading from top to bottom at the center of the figure.

C. Bubble-wall mode

In addition to the sub- and supercurvature modes, there is a contribution from the bubble-wall fluctuations. These fluctuations contribute as a transverse traceless curvature perturbation mode with $k^2 = -3$, see Refs. [15–17], which still behaves as a homogeneous random field [35,28].

Unlike the modes we have discussed so far, these modes need extra parameters for their description, because their amplitude depends on the details of the bubble-wall, which is determined by the potential for the σ field. This extra freedom allows the bubble-wall fluctuations to be tuned relative to the others.

The perturbation amplitude for the bubble-wall mode is given by [15,36,17]

$$A_W^2 = \frac{4U_T}{a^2 b m_{\text{Pl}}^4} [a^2 + (1+a^2 b)^2]^{1/2}, \quad (45)$$

where

$$a^2 = \frac{24\pi U_T S_1^2}{m_{\text{Pl}}^2 (U_F - U_T)^2}, \quad b = \frac{U_F - U_T}{4U_T}, \quad (46)$$

and S_1 gives the bubble-wall contribution to the bounce action, $B_{\text{wall}} = 2\pi^2 R^3 S_1$ (see, e.g., Ref. [15]). In order to compute S_1 , we will consider a symmetry-breaking potential of the type

$$U(\sigma) = U_F + \frac{\gamma}{4} \sigma^2 (\sigma - \sigma_0)^2 - \mu U_0 \left(\frac{\sigma}{\sigma_0} \right)^4, \quad (47)$$

where $\sigma_0 = M\sqrt{2/\gamma}$ corresponds to the true vacuum and $U_0 = M^4/16\gamma$ is the value of potential at the maximum. With $\mu \ll 1$ for the thin-wall approximation to be valid, S_1 can be computed as [15]

$$S_1 = \int_0^{\sigma_0} d\sigma [2(U(\sigma) - U_F)]^{1/2} \approx \frac{M^3}{3\gamma}. \quad (48)$$

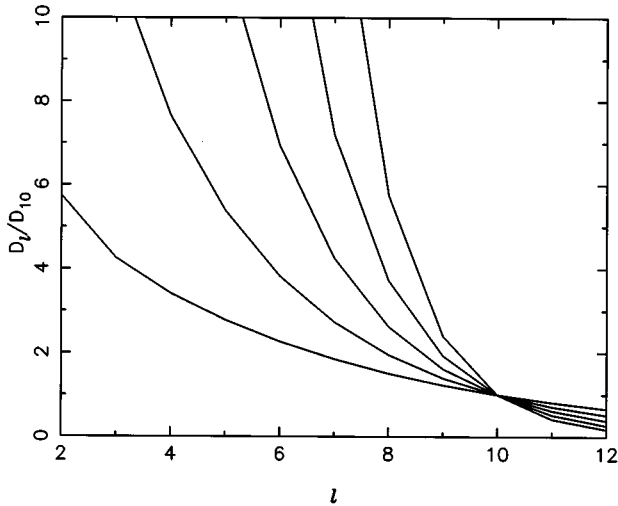


FIG. 3. As Fig. 1, but for the discrete bubble-wall mode, for $\Omega_0 = 0.6, 0.5, 0.4, 0.3, 0.2$, from top to bottom at low l .

In the limit $a^2 b \ll 1$ of small gravitational effects at tunneling, we recover the result of Ref. [8]; namely,

$$A_W^2 = \frac{2U_T(U_F - U_T)}{\pi m_{\text{pl}}^2 S_1^2} = A_C^2 \frac{3\epsilon}{2a^2 b}, \quad (49)$$

where ϵ is the slow roll parameter. However, in the opposite limit of strong gravitational effects, $a^2 b \gg 1$, we have [15]

$$A_W^2 = \frac{4U_T}{m_{\text{pl}}^4} = A_C^2 \frac{3\epsilon}{2}, \quad (50)$$

which is much smaller than the amplitude of the continuum modes.

The angular power spectrum associated with the bubble-wall mode is [15]

$$D_l^{(W)} \equiv l(l+1)C_l^{(W)} = \frac{4\pi A_W^2}{(l+2)(l-1)} \bar{W}_{2l}^2. \quad (51)$$

Figure 3 shows the first 12 multipoles. The quadrupole has the largest amplitude for all Ω_0 .

We will compare their contribution to the CMB in the next section.

V. COMPARISON WITH OBSERVATIONS

A. Microwave background anisotropies

We can now examine constraints on the shape of the combined spectrum. The COBE data alone do not offer particularly strong constraints in this respect; for example, although Yamamoto and Bunn [37] argued that the inclusion of supercurvature modes could harm the fit to COBE based on the two-year data, a recent comprehensive analysis of the four-year data by Górski *et al.* [38] finds no useful constraint. Those papers, however, discussed only a particular model for the supercurvature modes and did not include the bubble-wall modes at all. As Sasaki and Tanaka discussed [18], there can be interesting constraints if the supercurvature

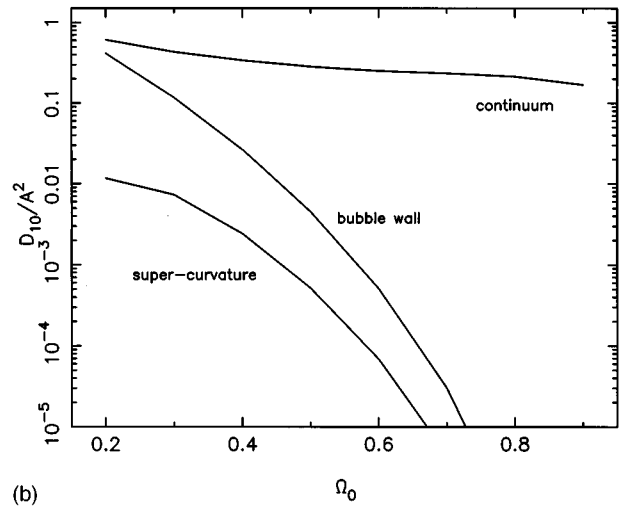
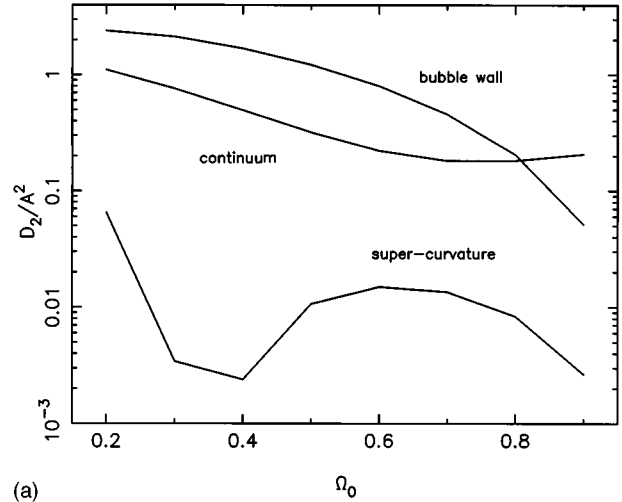


FIG. 4. The multipoles associated with each of the modes, normalized to the corresponding metric perturbation (A_C^2 , A_S^2 , or A_W^2 as appropriate), as a function of Ω_0 . The top panel shows the quadrupole, while the lower shows the tenth multipole.

modes have their amplitude enhanced, and we shall also see that the bubble-wall modes are typically more important than the supercurvature ones.

Unfortunately, the complicated structure of the perturbation spectra in open inflation models means that for a full analysis each model would have to be confronted with the COBE data set on a case-by-case basis. Such an analysis is outside the scope of this paper. We shall adopt a more simplistic approach, which is to demand that the discrete modes do not dominate the quadrupole while contributing negligibly to the tenth multipole. This would give an unacceptable shape to the spectrum on the scales sampled by COBE.

In Fig. 4, we show the contributions to the quadrupole and to the tenth multipole, as functions of Ω_0 , normalized to the size of the corresponding metric perturbation. It does not require much effort to keep the contribution to the tenth multipole from the discrete modes low (unless Ω_0 is very small), but we must ensure that the quadrupole is not dominated by the discrete modes.

Considering first the supercurvature modes, across the whole range of interesting Ω_0 , we find that the supercurva-

ture mode contributes about a factor 30 less to the low multipoles than do the continuum modes, for the same size of metric perturbation.² Unless Ω_0 is very small, and then if the supercurvature mode contribution is comparable to that of the continuum modes for the quadrupole, then it is negligible at the tenth multipole. Conservatively then, we shall require

$$A_S^2 \lesssim 100A_C^2, \quad (52)$$

independently of Ω_0 , to prevent the supercurvature modes from dominating the low multipoles. In principle, this limit could become inappropriate at small enough Ω_0 , because then the shape of the supercurvature spectrum is not so steep as to be ruled out by observations. However, by then the supercurvature modes are contributing substantially even to the tenth multipole, and this will force down the normalization of COBE and make it impossible to fit large-scale structure observations. We can, therefore, adopt the above constraint even at low Ω_0 values. This imposes only a very mild constraint on the parameters of the model, namely,

$$\alpha > 0.01, \quad (53)$$

which is easy to satisfy as we will see in Sec. VI. Since the value of Ω_0 at present is not known with any reasonable accuracy, it would be excessive to give a precise Ω_0 -dependent constraint. However, in the future, with a narrow range of values for Ω_0 , one would be able to give a more refined constraint on the parameters of the model from a full comparison of the detailed spectrum against COBE or its successors.

The same arguments can be applied to the bubble-wall modes; again, we must prevent the domination of the quadrupole by these modes. For the interesting Ω_0 values (i.e., those not too close to 1), we see from Fig. 4 that this simply requires

$$A_W^2 \lesssim A_C^2, \quad (54)$$

again independent of Ω_0 in the interesting range. This again imposes only a very mild constraint on the parameters of the model. For $a^2b \ll 1$, we have $3\epsilon < 2a^2b$, giving

$$\gamma < 9 \times 10^4 \frac{1 + 6\xi M^3}{6\xi m_{\text{pl}}^3} \alpha^{5/2}, \quad (55)$$

which is easy to satisfy for sufficiently large M . For $a^2b \gg 1$, the amplitude of the metric perturbation, Eq. (50), is completely negligible since $\epsilon \ll 1$, see Sec. VI.

B. Implications for large-scale structure

We can now combine the COBE normalization with observations of large-scale structure. This has the advantage of being relatively insensitive to the inclusion of supercurvature or bubble-wall modes, because with the constraints above

these modes affect only the lowest multipoles, and while these can influence whether or not the spectral shape is a good fit to observations, they are not very significant at the higher multipoles (around the 10th to 15th) which are most important for determining the normalization. The drawback though is that looking to large-scale structure introduces a dependence on all the other cosmological parameters, namely, the Hubble parameter h , the baryon density Ω_B , and the nature of the dark matter. Despite this, interesting constraints can still be found, and two analyses have appeared which discuss tilted open models — Liddle *et al.* [39] who used the two-year COBE data and, more recently, White and Silk [40] who used an accurate normalization to the four-year COBE data. Both of these considered only cold dark matter; other choices tend to strengthen the constraints so we shall do likewise.

In the model we are considering, the spectral index is always tilted to n less than one, as seen from Eq. (35). Whether or not this is allowed depends quite sensitively on both Ω_0 and h . If Ω_0 is too low, below around 0.30, then the open cold dark matter model fares badly against observations; this conclusion is consistent with a similar constraint from velocity flows [41] which is independent of the power spectrum. For example, White and Silk [40] find that this value is allowed only if the power spectrum is “blue,” with n at least 1.10. This conclusion is enforced both by the cluster abundance and by the shape of the galaxy correlation function. Our model will, therefore, be ruled out if it turns out that the universe is indeed as open as this.

However, one does not have to increase Ω_0 by very much to radically change this conclusion. For $\Omega_0 = 0.5$, for example, White and Silk find viable models for n as low as 0.85, with the preferred value depending on the Hubble parameter h . Our model can, therefore, be comfortably compatible with the data for this Ω_0 , and at least marginally compatible for Ω_0 as low as 0.4.

VI. TWO POSSIBLE SCENARIOS

In this section we will explore two different scenarios.

A. $\xi \ll 1$

This case was considered in Ref. [20]. Here, the dilaton expectation value ν is much larger than the present Planck mass, see Eq. (8). For definiteness, we will choose a particular value, $8\xi = 1/200$. From the required number of e -folds, Eq. (28), this determines α to be of order one.

Let us study now the contribution of the different modes to the CMB anisotropies. We first consider the continuum spectrum of subcurvature modes. The slow roll parameters, given by Eqs. (25) and (26), become

$$\epsilon \approx \frac{1}{200}, \quad \eta \approx 0, \quad (56)$$

which determine the tilt of the primordial spectrum of density perturbations via Eq. (35) as

$$n - 1 \approx -6\epsilon \approx -0.03, \quad (57)$$

²Although there is a dip around $\Omega_0 \approx 0.4$, caused by an “accidental” cancellation between intrinsic and line-of-sight terms, the dip is not at the same location for the $l = 3, 4, \dots$ multipoles so the dip does not allow one to weaken the constraint in its neighborhood [34].

which is compatible with large- and small-scale observations for $\Omega_0 \gtrsim 0.4$, according to Ref. [40]. The constraint on the amplitude of the angular power spectrum determines the value of λ via Eq. (41) as

$$\lambda \approx 2.5 \times 10^{-5} \frac{6\xi^3}{1+6\xi} \approx 4 \times 10^{-14}. \quad (58)$$

See Ref. [20] for a range of values, under the assumption $\xi \ll 1$.

We now consider the de Sitter vacuum supercurvature mode. This mode exists, since $m_F^2 < 2H_F^2$ for $\xi \ll 1$ from Eqs. (18) and (19). The amplitude of curvature perturbations that give rise to temperature anisotropies in the CMB is constrained by Eq. (52), which imposes the condition equation (53). This is satisfied as long as $\alpha > 0.01$. Since we are considering values of $\alpha \approx 1$, the contribution from the supercurvature mode will be negligible compared to that of the subcurvature modes, regardless³ of Ω_0 .

Consider now the bubble-wall mode contribution to the CMB anisotropies. There are two possibilities, depending on the relative strength of the gravitational effects at tunneling [15]. For $a^2 b \ll 1$ we are in the weak gravity regime of Ref. [8], and the condition on the parameters becomes, from Eq. (55),

$$\gamma < 10^5 \frac{1+6\xi}{6\xi} \frac{M^3}{m_{\text{Pl}}^3}. \quad (59)$$

For $M \approx 10^{-3} m_{\text{Pl}}$, this gives $\gamma < 0.03$, which is a reasonable bound on the coupling γ . On the other hand, for $a^2 b \gg 1$, condition equation (54) is easily satisfied for $\epsilon \approx 1/200$, see Eq. (50).

B. $\xi \gg 1$

This case was considered in Ref. [42]. The dilaton expectation value ν is much smaller than the present Planck mass. For $\xi \gg 1$, we have $\beta \approx 4/3$ and the value of α is now determined from the required number of e -folds, Eq. (28),

$$\frac{4N}{3} \approx \alpha - \frac{4}{3} - \ln\left(\frac{1+\alpha}{1+4/3}\right), \quad (60)$$

which gives $\alpha \approx 85$. This is a regime quite different from the previous case.

We first consider the continuum spectrum of subcurvature modes. The slow-roll parameters are

$$\epsilon \approx 1.85 \times 10^{-4}, \quad \eta \approx -0.016, \quad (61)$$

which determine the tilt of the primordial spectrum of density perturbations via Eq. (35) as

$$n-1 \approx 2\eta \approx -0.032. \quad (62)$$

This is very similar to the previous case and thus compatible with large- and small-scale observations for $\Omega_0 \gtrsim 0.4$. How-

³In the limit of small α and β , the e -foldings relation, Eq. (28), gives $\alpha \approx 10\sqrt{\beta}$, so the supercurvature constraint will eventually become important once $\xi \lesssim 10^{-7}$.

ever, the constraint on the amplitude of the angular power spectrum now determines the value of the combination λ/ξ^2 rather than λ alone, as

$$\frac{\lambda}{\xi^2} \approx 9 \times 10^{-10}. \quad (63)$$

If we choose $\lambda \sim 1$, we have $\xi \sim 3 \times 10^4$, which gives a very reasonable expectation value for the dilaton, from Eq. (8), of

$$\nu \approx 10^{-3} m_{\text{Pl}} \approx 10^{16} \text{ GeV}. \quad (64)$$

We now consider the de Sitter vacuum supercurvature mode. This mode also exists in this case, since $m_F^2 < 2H_F^2$ for $\alpha \gg 1$ from Eqs. (18) and (19). The amplitude of curvature perturbations is constrained by Eq. (52), which imposes the condition equation (53). Since we have $\alpha \gg 1$, the contribution from this supercurvature mode will be negligible.

Concerning the bubble-wall mode contribution, again there are two possibilities. In the weak gravity regime $a^2 b \ll 1$, the condition on the parameters becomes

$$\gamma < 10^5 \frac{M^3}{m_{\text{Pl}}^3} \alpha^{5/2}, \quad (65)$$

which gives a trivial constraint of $\gamma \lesssim 7$ for $M \approx 10^{-3} m_{\text{Pl}}$. For $a^2 b \gg 1$, the condition in Eq. (54) is easily satisfied for $\epsilon \approx 10^{-4}$.

VII. MATTER ERA

One of the remaining issues is to make sure that after inflation the scalar field φ remains close to the minimum of its potential. Deviations from this would result in time variations of the gravitational constant, which are strongly constrained [43]. During the radiation era the scalar field will remain at the minimum due to the vanishing trace of the energy-momentum tensor, as seen from Eq. (6). However, during the matter era the dilaton couples to the matter fluid and thus will be subject to a force which shifts the field from its minimum.

However, it is easy to show that this effect is tiny. The relevant equation, from Eq. (6), is

$$\ddot{\varphi} + 3H\dot{\varphi} + \frac{\dot{\varphi}^2}{\varphi} = \frac{4V(\varphi) - \varphi V'(\varphi) + \rho}{(1+6\xi)\varphi}. \quad (66)$$

For a given ρ , there is a static solution at

$$\varphi_{\text{st}}^2 = \nu^2 \left(1 + \frac{2\rho}{\lambda \nu^4} \right). \quad (67)$$

Since the matter-era energy density is tiny in comparison to the inflationary energy density which determines $\lambda \nu^4$, the fractional shift in the gravitational constant at this static point is tiny, and so too is the energy density associated with the potential, which contributes only a minute fraction (perhaps 10^{-100}) of the critical density.

We have analyzed the detailed behavior, described in Appendix B. When matter domination starts, the field rises from its minimum to oscillate about the static point, which it does on a very rapid time scale. As ρ decreases, the static point

moves towards the true minimum (with the oscillation amplitude also decreasing though rather more slowly). At all times, the oscillations are of such small amplitude that general relativity holds to extremely high accuracy.

VIII. CONCLUSIONS

In this paper we have analyzed a variety of phenomenological constraints on a recently proposed model of open inflation in the context of induced gravity theories [20]. The most stringent constraints come from observations of the temperature anisotropies in the microwave background. The model predicts a matter power spectrum tilted to $n < 1$, which will be incompatible with observations if the universe turns out to have $\Omega_0 \leq 0.4$. Otherwise, it is possible to choose the parameters of the model so that it is in agreement with observations.

During the matter era, the large dilaton mass and the extremely small amplitude of oscillations around its vacuum expectation value ensure that the theory approaches general relativity very efficiently, passing all the post-Newtonian and oscillating gravitational coupling tests.

Note added. We commented in the introduction that our method had been formulated to compute the gravitational wave spectrum, which we, therefore, did not consider. As we were revising for the final version of this paper, papers appeared [44] making significant progress in this direction. These new results have been applied to the model discussed in this paper in Ref. [45], which confirms compatibility with observations.

ACKNOWLEDGMENTS

J.G.B. was supported in part by PPARC and A.R.L. by the Royal Society. We thank Anne Green, Andrei Linde, and Martin White for useful discussions. J.G.B. thanks Stanford University for its hospitality during part of this work, with the visit funded by NATO Collaborative Research Grant Ref. CRG.950760.

APPENDIX A: OPEN UNIVERSE MODE FUNCTIONS

The open universe mode functions are discussed in Refs. [14,28].

1. Subcurvature modes

The subcurvature modes can be written as [46,14]

$$\Pi_{ql}(r) = N_{ql} \tilde{\Pi}_{ql}(r), \quad (\text{A1})$$

with

$$N_{ql} = \sqrt{\frac{2}{\pi}} \prod_{n=1}^l (n^2 + q^2)^{-1/2}, \quad N_{q0} = \sqrt{\frac{2}{\pi}}, \quad (\text{A2})$$

where the unnormalized modes $\tilde{\Pi}_{ql}(r)$ can be generated from the first two

$$\tilde{\Pi}_{q0}(r) = \frac{\sin qr}{\sinh r}, \quad (\text{A3})$$

$$\tilde{\Pi}_{q1}(r) = \frac{\coth r \sin qr - q \cos qr}{\sinh r}, \quad (\text{A4})$$

through the recurrence relation

$$\tilde{\Pi}_{ql}(r) = (2l-1) \coth r \tilde{\Pi}_{q,l-1}(r) - [(l-1)^2 + q^2] \tilde{\Pi}_{q,l-2}(r). \quad (\text{A5})$$

2. Supercurvature modes

The first ($l \geq 1$) multipoles are [34]

$$\bar{\Pi}_{11}(r) = \frac{1}{2} \left[\coth r - \frac{r}{\sinh^2 r} \right], \quad (\text{A6})$$

$$\bar{\Pi}_{12}(r) = \frac{1}{2} \left[1 + \frac{3(1 - r \coth r)}{\sinh^2 r} \right]. \quad (\text{A7})$$

The rest can be obtained with the recurrence relation

$$\bar{\Pi}_{1l}(r) = \frac{2l-1}{l-1} \coth r \bar{\Pi}_{1,l-1}(r) - \frac{l}{l-1} \bar{\Pi}_{1,l-2}(r). \quad (\text{A8})$$

3. Bubble-wall modes

The first ($l \geq 2$) multipoles are [15]

$$\bar{\Pi}_{22}(r) = \frac{\sinh 4r - 8 \sinh 2r + 12r}{4 \sinh^3 r}, \quad (\text{A9})$$

$$\bar{\Pi}_{23}(r) = \frac{\sinh 5r - 15 \sinh 3r - 80 \sinh r + 120r \cosh r}{8 \sinh^4 r}. \quad (\text{A10})$$

The rest can be obtained from the recurrence relation

$$\bar{\Pi}_{2l}(r) = \frac{2l-1}{l-2} \coth r \bar{\Pi}_{2,l-1}(r) - \frac{l+1}{l-2} \bar{\Pi}_{2,l-2}(r). \quad (\text{A11})$$

APPENDIX B: MATTER-ERA OSCILLATIONS OF THE GRAVITATIONAL COUPLING

Here, we carry out a detailed analysis of the evolution of the dilaton during the radiation and matter eras. Here, we shall assume that the oscillations are damped only by the Hubble expansion and not by any particle decays, if such decays were present the general relativistic limit would be even more quickly approached.

The energy-momentum tensor conservation equation (5) in the Jordan frame ensures $\rho a^{3(1+w)} = \text{const}$ during the radiation ($w = 1/3$) and matter ($w = 0$) eras. In order to study the cosmological evolution during these eras, let us redefine our variables as

$$u = \frac{\varphi^2}{\nu^2} - 1, \quad z = mt, \quad (\text{B1})$$

where m is given by

$$m^2 = \frac{\lambda \nu^2}{1 + 6\xi}. \quad (\text{B2})$$

The φ equation of motion, Eq. (6), and the Friedman equation become

$$u'' + 3\frac{a'}{a}u' + u = \frac{2(\rho - 3p)}{\lambda v^4}, \quad (\text{B3})$$

$$\left[2\frac{a'}{a} + \frac{u'}{1+u}\right]^2 = \frac{1+6\xi}{6\xi} \left[\left(\frac{u'}{1+u}\right)^2 + \frac{u^2}{1+u} + \frac{8\rho}{\lambda v^4(1+u)} \right], \quad (\text{B4})$$

where primes denote derivatives with respect to z . During the radiation era, the right-hand side of Eq. (B3) vanishes and $u = u' = 0$ is a stable fixed point. Very soon one can neglect the u terms in the Friedman equation, and we find the radiation era attractor, $a'/a = 1/2z$. The scalar field equation of motion, $u'' + 3u'/2z + u = 0$, has an exact solution:

$$z^{1/4}u(z) = c_1 J_{1/4}(z) + c_2 Y_{1/4}(z), \quad (\text{B5})$$

where $\{J, Y\}$ are Bessel functions. Its amplitude decays asymptotically as $u(z) \propto z^{-3/4}$, so we expect the matter era to start with initial conditions at $u = u' = 0$.

During the matter era, $u = u' = 0$ is a spiral attractor and we can always neglect the u terms in the Friedman equation:

$$\left(\frac{a'}{a}\right)^2 \simeq \left(\frac{1+6\xi}{6\xi}\right) \frac{A}{a^3} = \frac{4}{9z^2}, \quad (\text{B6})$$

where $A = 2\rho a^3/\lambda v^4$ is a constant of order 10^{-120} in Planck units. The equation of motion for u becomes

$$u'' + \frac{2}{z}u' + u = \frac{A}{a^3} = \frac{K}{z^2}, \quad (\text{B7})$$

where $K = \beta/3$, see Eq. (27). There is an exact solution,

$$zu(z) = c_1 \text{sinc}z + c_2 \text{cosc}z + Kf(z), \quad (\text{B8})$$

where $f(z)$ is related to the sine and cosine integral functions by [47]

$$f(z) = \text{Ci}(z)\text{sinc}z - \text{Si}(z)\text{cosc}z = \int_0^\infty \frac{e^{-zt}}{1+t^2} dt. \quad (\text{B9})$$

The late time ($z \rightarrow \infty$) behavior of u is $u(z) \propto \text{sinc}z/z$, with a large frequency of oscillations

$$m = \left[\frac{\lambda}{8\pi\xi(1+6\xi)} \right]^{1/2} m_{\text{Pl}} \gg H_0, \quad (\text{B10})$$

and an amplitude $|u'| \sim |u| \sim A/a_0^3$, which later decays as $1/z$ at large z . The contribution of the scalar field to the total energy density is, therefore, suppressed by an extra factor A with respect to the ordinary matter energy density, see Eq. (B4). Since A is so tiny, there are no constraints on the parameters of the model from local experiments, see Ref. [25], and general relativity is a strong attractor of the equations of motion.

Note that during the matter era the background dilaton field oscillates very quickly, which might be thought could produce other particles, such as at the end of inflation. However, because of the extremely small amplitude of oscillations, $|u| \sim A \sim 10^{-120}$, there is no significant particle production and the field's energy can only decay by redshifting away.

-
- [1] A. D. Linde, *Particle Physics and Inflationary Cosmology* (Harwood, Chur, Switzerland, 1990).
- [2] C. L. Bennett *et al.*, *Astrophys. J.* **464**, L1 (1996).
- [3] MAP home page at <http://map.gsfc.nasa.gov/> (1997).
- [4] Planck home page at <http://astro.estec.esa.nl/SA-general/Projects/Cobras/cobras.html> (1997).
- [5] G. Jungman, M. Kamionkowski, A. Kosowsky, and D. N. Spergel, *Phys. Rev. D* **54**, 1332 (1996).
- [6] J. R. Gott, *Nature (London)* **295**, 304 (1982); M. Sasaki, T. Tanaka, K. Yamamoto, and J. Yokoyama, *Phys. Lett. B* **317**, 510 (1993).
- [7] M. Bucher, A. S. Goldhaber, and N. Turok, *Phys. Rev. D* **52**, 3314 (1995); M. Bucher and N. Turok, *ibid.* **52**, 5538 (1995).
- [8] A. D. Linde, *Phys. Lett. B* **351**, 99 (1995); A. D. Linde and A. Mezhlumian, *Phys. Rev. D* **52**, 6789 (1995).
- [9] W. L. Freedman *et al.*, *Nature (London)* **371**, 757 (1994); N. R. Tanvir, T. Shanks, H. G. Ferguson, and D. R. T. Robinson, *ibid.* **377**, 27 (1995).
- [10] J. García-Bellido, in *TAUP '95*, Proceedings of the International Symposium on Theoretical and Phenomenological Aspects of Underground Physics, Toledo, Spain, edited by A. Morales *et al.* [*Nucl. Phys. B (Proc. Suppl.)* **48**, 128 (1996)]; J. D. Cohn, Berkeley Report No. astro-ph/9606052, 1996 (unpublished).
- [11] D. H. Lyth and E. D. Stewart, *Phys. Lett. B* **252**, 336 (1990).
- [12] B. Ratra and P. J. Peebles, *Phys. Rev. D* **52**, 1837 (1995).
- [13] M. Sasaki, T. Tanaka, and K. Yamamoto, *Phys. Rev. D* **51**, 2979 (1995).
- [14] D. H. Lyth and A. Woszczyna, *Phys. Rev. D* **52**, 3338 (1995).
- [15] J. García-Bellido, *Phys. Rev. D* **54**, 2473 (1996).
- [16] J. Garriga, *Phys. Rev. D* **54**, 4764 (1996).
- [17] K. Yamamoto, M. Sasaki, and T. Tanaka, *Phys. Rev. D* **54**, 5031 (1996).
- [18] M. Sasaki and T. Tanaka, *Phys. Rev. D* **54**, R4705 (1996).
- [19] A. R. Liddle and D. H. Lyth, *Phys. Lett. B* **291**, 391 (1992).
- [20] A. M. Green and A. R. Liddle, *Phys. Rev. D* **55**, 609 (1997).
- [21] A. Zee, *Phys. Rev. Lett.* **42**, 417 (1979).
- [22] C. Brans and R. H. Dicke, *Phys. Rev.* **124**, 925 (1961).
- [23] S. Weinberg, *Gravitation and Cosmology* (Wiley, San Francisco, 1972).
- [24] J. García-Bellido and A. D. Linde, *Phys. Rev. D* **52**, 6730 (1995).
- [25] P. J. Steinhardt and C. M. Will, *Phys. Rev. D* **52**, 628 (1995).
- [26] J. R. Gott and T. S. Statler, *Phys. Lett.* **136B**, 157 (1984).
- [27] F. S. Accetta, D. J. Zoller, and M. S. Turner, *Phys. Rev. D* **31**, 3046 (1985).
- [28] J. García-Bellido, A. R. Liddle, D. H. Lyth, and D. Wands, preceding paper, *Phys. Rev. D* **55**, 4596 (1997).

- [29] R. K. Sachs and A. M. Wolfe, *Astrophys. J.* **147**, 73 (1967).
- [30] V. F. Mukhanov, H. A. Feldman, and R. H. Brandenberger, *Phys. Rep.* **215**, 203 (1992).
- [31] A. R. Liddle and D. H. Lyth, *Phys. Rep.* **231**, 1 (1993).
- [32] E. F. Bunn, D. Scott, and M. White, *Astrophys. J.* **441**, L9 (1995).
- [33] E. F. Bunn and M. White, *Astrophys. J.* (to be published).
- [34] J. García-Bellido, A. R. Liddle, D. H. Lyth, and D. Wands, *Phys. Rev. D* **52**, 6750 (1995).
- [35] T. Hamazaki, M. Sasaki, T. Tanaka, and K. Yamamoto, *Phys. Rev. D* **53**, 2045 (1996).
- [36] J. D. Cohn, *Phys. Rev. D* **54**, 7215 (1996).
- [37] K. Yamamoto and E. F. Bunn, *Astrophys. J.* **461**, 8 (1996).
- [38] K. Górski, B. Ratra, R. Stompor, N. Sugiyama, and A. J. Banday, Max Planck Report No. astro-ph/9608054, 1996 (unpublished).
- [39] A. R. Liddle, D. H. Lyth, D. Roberts, and P. T. P. Viana, *Mon. Not. R. Astron. Soc.* **278**, 644 (1996).
- [40] M. White and J. Silk, *Phys. Rev. Lett.* **77**, 4704 (1996).
- [41] A. Dekel, *Annu. Rev. Astron. Astrophys.* **32**, 371 (1994).
- [42] B. Spokoiny, *Phys. Lett.* **129B**, 39 (1984).
- [43] C. M. Will, *Theory and Experiment in Gravitational Physics* (Cambridge University Press, Cambridge, England, 1993).
- [44] T. Tanaka and M. Sasaki, Osaka Report No. astro-ph/9701053, 1997 (unpublished); M. Bucher and J. D. Cohn, Stony Brook Report No. astro-ph/9701117, 1997 (unpublished).
- [45] J. García-Bellido, CERN Report No. astro-ph/9702211, 1997 (unpublished).
- [46] E. R. Harrison, *Rev. Mod. Phys.* **39**, 862 (1967); M. L. Wilson, *Astrophys. J.* **273**, 2 (1983); L. F. Abbott and R. K. Schaefer, *ibid.* **308**, 546 (1986).
- [47] *Handbook of Mathematical Functions*, edited by M. Abramowitz and I. A. Stegun (Dover, New York, 1964), p. 232.